Percolation process on the superconducting paths in $Y_{1-x}Pr_xBa_2Cu_3O_{7-\delta}$

Katsukuni Yoshida
Department of Fundamental Energy Science, Graduate School of Energy Science, Kyoto University, Uji, Kyoto-fu, Japan 611-0011
(Received 2 December 1998)

In the compound $Y_{1-x}Pr_xBa_2Cu_3O_{7-\delta}$, a two-dimensional site-percolation system of the square lattice is realized with structural elements of Y-sited and Pr-sited crystal unit cells. The diamagnetic behavior at temperatures as low as 4.2 K has revealed that superconductivity is featured by the several characteristic points in the range of Pr concentration (x): the first percolation threshold $x_{pc1}=0.41$, the second one $x_{pc2}=0.59$, and virtual thresholds $x_1=0.44$ and $x_2=0.55$. At these points the superconducting path changes in its structure. In the range $x_2 \geqslant x \geqslant x_1$, the path becomes fragile, largely depending on the magnetic field h(ac). The presence of x_2 implies that the isolated Y-sited unit cell is assimilated into the adjacent Pr-sited cells, and so the percolation threshold is shifted from the true one x_{pc2} to the virtual one x_2. If this effect occurs also to the isolated Pr-sited unit cell, then x_1 becomes a virtual threshold stemming from x_{pc1}. [S0163-1829(99)05234-0]

Among the lanthanoid cuprates as represented by $YBa_2Cu_3O_{7-\delta}$ (YBCO), the Pr-based cuprate $PrBa_2Cu_3O_{7-\delta}$ (PBCO) is left out of the group, since it exhibits neither superconductivity nor metallic conduction, but remains an antiferromagnetic insulator. How to explain the suppression of the superconductivity in PBCO has been a hot issue, discussed by using a variety of models.[1,2] From the nature of PBCO, doping of YBCO with Pr is normally expected to degrade the initial superconductivity of YBCO.[3–5] The crystal structure of PBCO is isomorphic to that of YBCO, with Pr and Y being substitutable at the same site. By virtue of this crystallography, the compound $Y_{1-x}Pr_xBa_2Cu_3O_{7-\delta}$ can be a mixed crystalline composite consisting of two kinds of structural elements of the Y-sited unit cell (YBCO) and the Pr-sited unit cell (PBCO), as depicted in Fig. 1. This composite has been found to realize a percolation system with the critical points (thresholds) $x_{c1}=0.46$ and $x_{c2}=0.58$, as investigated by Muroi and Street.[6] Its high structural resolution of the same order as the lattice constants is mainly due to the extremely short coherence length. This system has two-dimensional (2D) characteristics, since its superconductivity is substantially confined within the CuO_2 plane. Such a percolation model has also been applied to other doped cuprates, as reported earlier by Govea *et al.*[7] However, it is ambiguous as to whether this percolation system can be such a classic one as is simply constructed by the structural elements, the identity of which always remains unchanged. This question rises from whether the electronic identity of the Y-sited unit cell can be lost by adjoining the Pr-sited unit cells. With this problem in mind, we have investigated the electrical and diamagnetic properties of $Y_{1-x}Pr_xBa_2Cu_3O_{7-\delta}$. In the following, the Y-sited unit cell and Pr-sited unit cell will be called simply the Y cell and Pr cell.

A series of $Y_{1-x}Pr_xBa_2Cu_3O_{7-\delta}$ (YPBCO) samples was synthesized by the solid reaction method from a stoichiometric mixture of Y_2O_3, Pr_6O_{11}, $BaCO_3$, and CuO, through the repeated processes of grinding and subsequent calcining at 900 °C in air. The fabrication process was completed by sintering at 960 °C and subsequent annealing at 500 °C in an oxygen atmosphere. The Pr concentration x was varied in the range $0.6 \geqslant x \geqslant 0$. The electrical resistivity was measured by the conventional four-probe configuration and the diamagnetic susceptibility was measured by an ac method using induction coils. The samples were shaped in almost the same size with typical dimensions of $1.50 \times 0.61 \times 0.12$ cm^3.

Figure 2 shows the temperature dependence of the resistivity ρ. As reported in early investigations,[3–5] the doping with Pr results in the degradation of the superconductivity. Both the zero-resistance temperature and the onset temperature decrease monotonically with increasing x, and accordingly, the resistance in the normal region increases. When x exceeds about 0.5, an upward deviation from the linearity becomes distinct, and after passing the maximum the resistivity turns downward to zero resistance with decreasing T. Eventually, the superconductor-insulator transition takes place at $x \approx 0.6$, giving ρ as a monotonically decreasing function of T. The dependence on the current density J becomes obvious for $x=0.55$, as will be discussed later.

Figure 3 displays the temperature dependence of the diamagnetic susceptibility χ (real part of the ac susceptibility) for different x. The diamagnetism is affected by the magnetic field h (ac), where h was applied by the ac current supplied for measuring the inductance of the samples placed in a coil. As x increases, the effect of h on χ becomes stronger, and it appears different according to x on the low-temperature side. At a low concentration with $x=0.35$, the curves converge at 4.2 K, showing full recovery of the superconductivity, while for a high concentration with $x=0.5$ the recovery vanishes. This recovery reflects the tolerance of the superconducting path to h. From the above comparison, there must be a critical point of x at which the diamagnetic recovery changes its behavior. From the percolation model,[8] this point is expected to be the first percolation threshold $x_{pc1}=0.41$ (or $y_{pc1}=1-x_{pc1}=0.59$ in terms of Y concentration) of the 2D site percolation on the square lattice. For $x<x_{pc1}$, the superconducting cluster is formed only by the connection between the nearest-neighbor Y cells, and so x_{pc1} (or y_{pc1}) is referred to as the first percolation threshold.

Straddling this threshold x_{pc1}, we can see two types of superconducting paths, as depicted in Fig. 1(c). At low concentrations ($x<x_{pc1}$), the path is made of such Y cells join-

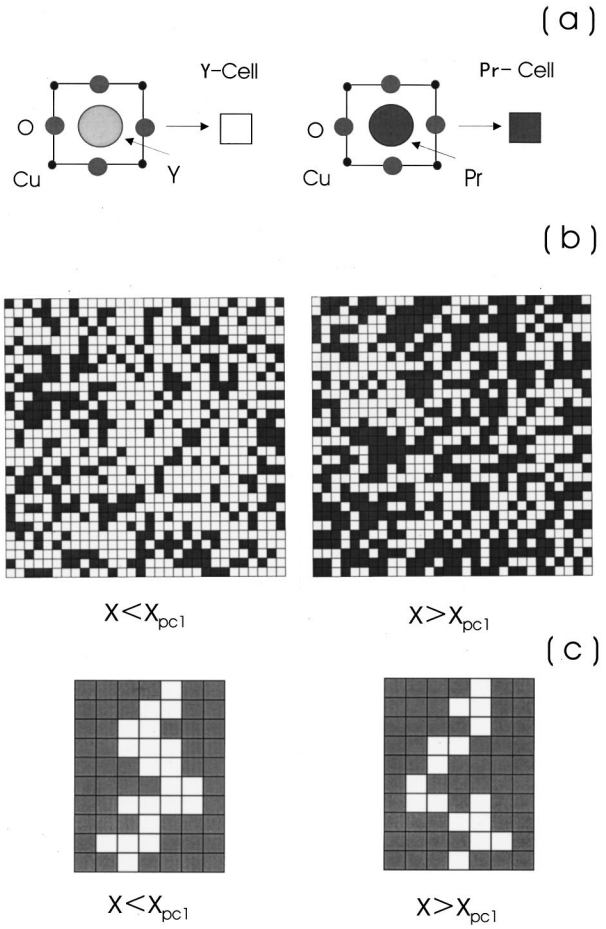

FIG. 1. (a) Y-sited unit cell (YBCO, light square) and Pr-sited unit cell (PBCO, dark square), viewed from the *c*-axis direction perpendicular to the CuO_2 plane; (b) the structures at $x=0.35$ and 0.52, distinguished by the first percolation threshold x_{pc1}; and (c) the corresponding current paths.

ing each other at their lateral faces. Its superconductivity has a high tolerance to the field *h*, and so a strong recovery of the diamagnetism is realized for this type of path. On the high-concentration side ($x>x_{pc1}$), the superconducting path changes in its structure, as shown in Fig. 1(c). The structure is built by joining Y cells at the corners of each cell in addition to the connection at the lateral face; that is, the path is formed not only by the first nearest-neighbor connection but also by the second nearest-neighbor one. The superconducting current passes through the corner connection by virtue of the weak-link-like Josephson coupling, and is fragile to the field *h*. The degradation in diamagnetic recovery reflects this fragile structure. This structure is expected to persist until *x* attains another threshold $x_{pc2}=0.59$, at which time the superconducting path spanning the overall system is broken, giving rise to the superconductor-insulator transition. The point x_{pc2} (or $y_{pc2}=0.41$) is called below the second percolation threshold, since the connection between the second nearest-neighbor Y cells determines x_{pc2}.[8]

From the above model, the second type of superconducting path, which is sensitive to *h*, is expected to be formed in the specified range $x_{pc2}\geqslant x\geqslant x_{pc1}$. We examine this prediction on the *x* dependence curves of χ for different *h*. Figure 4 displays the result at $T=4.2$ K. At around the concentration $x=0.42$, which approximates to x_{pc1}, the curves begin to rise, showing a precursor change in the path structure, but only with a trivial dependence on *h* until *x* attains $x_1=0.44$. When *x* exceeds x_1, the curves begin to rise steeply and exhibit a large dependence on *h*. This steep rise will refer to the upward deviation from the linearity of ρ, since the value of x_1 approximates to $x_{c1}=0.46$, at which the deviation was observed to start.[6] The considerable dependence on *h* indicates that the second type of superconducting path governed by the weak link appears only in the range $x_2\geqslant x\geqslant x_1$, which is narrower than the expected range $x_{pc2}\geqslant x\geqslant x_{pc1}$. Of interest is that both the *x* dependence and the *h* dependence substantially disappear when *x* exceeds $x_2=0.55$. From the usual percolation theory, such a critical point should be the second percolation threshold $x_{pc2}=0.59$ instead of x_2. This variance means that the superconducting path spanning overall the system is virtually broken in spite of *x* less than x_{pc2}.

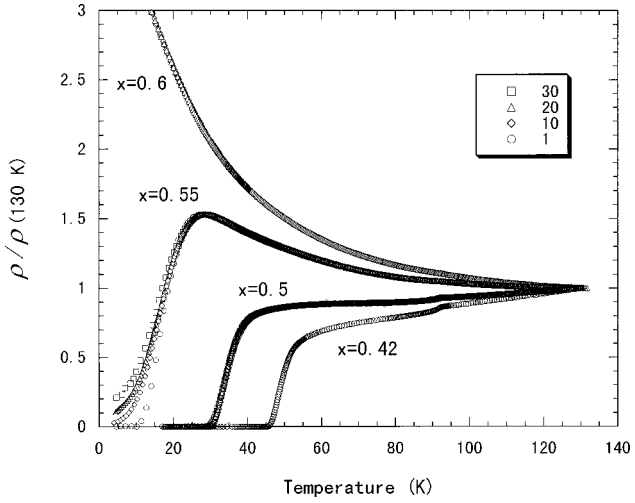

FIG. 2. Temperature dependence of the resistivity ρ on varying *x* in zero magnetic field. The legend indicates the current density *J*: (1,10, 20, 30) refer to (0.014, 0.14, 0.28, 0.42 A/cm^2).

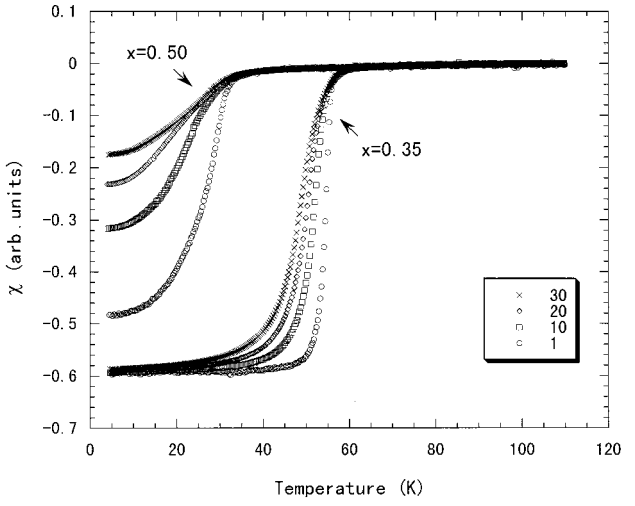

FIG. 3. Temperature dependence of the diamagnetic susceptibility χ when the magnetic field h(ac) is increased. The legend indicates the magnetic field *h*: (1,10,20,30) refer to [0.1, 1, 2, 3 Oe (rms)].

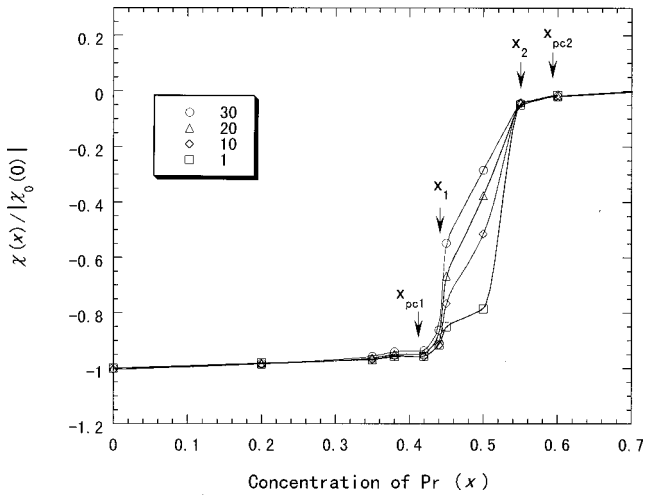

FIG. 4. Pr-concentration dependence of the diamagnetic susceptibility χ at $T=4.2$ K on varying field h; χ is normalized with the absolute value of χ_0 at $x=0$ and $h=0.1$ Oe. The legend indicates the magnetic field h: (1,10,20,30) refer to [0.1, 1, 2, 3 Oe (rms)]. The arrows indicate the first and second percolation thresholds (x_{pc1}, x_{pc2}) and virtual thresholds (x_1, x_2).

The basic pattern of the χ vs x curves was observed to be almost unchanged even at $T=20$ K, giving the same values of x_1 and x_2; however, the pattern changed obviously at higher temperatures.

From the above observation, it seems natural to pursue the origin which is unaffected by T and h for explaining the thresholds x_1 and x_2, and so let us consider the behavior of the structural elements themselves rather than that of the Josephson tunneling or the order parameter. Figure 5 depicts the distribution of Y cells of type Y_n classified by the number of adjacent Y cells at the lateral face. The distribution was calculated for a computer-generated site-percolation system on a square lattice of a size of 500×500, with the periodic boundary condition being used. In the range $x_{pc2}\geqslant x$

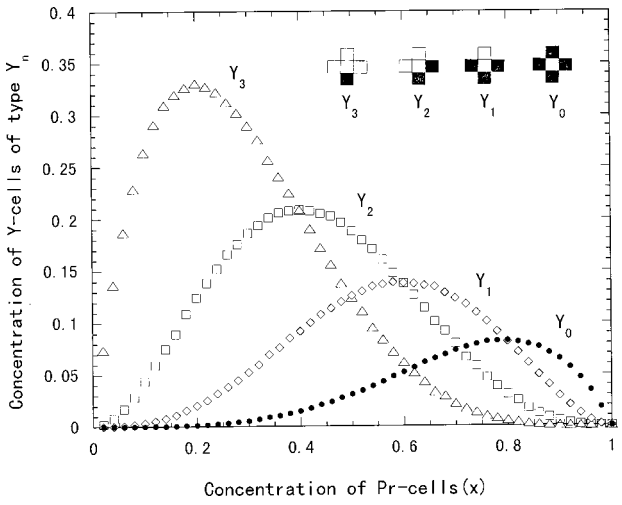

FIG. 5. Distribution of the Y cells adjoining the Pr cells (dark squares) on the square lattice with size 500×500. In the inset, as denoted by Y_n ($n=0-3$), the centered Y cell is classified according to the number n of the adjoining Y cells (light squares). The calculation used a periodic boundary condition.

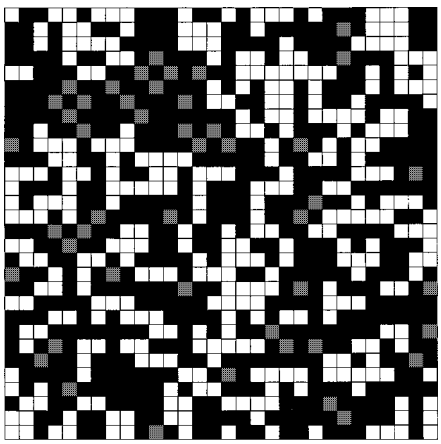

FIG. 6. The 2D site percolation structure ($x=0.56$) when $x_{pc2}>x>x_2$, where the isolated Y_0 cells (gray squares) become ineffective in the superconductivity, and so the overall spanning of the superconducting path (light part) is violated.

$\geqslant x_{pc1}$, a large number of the highly adjoining cells Y_3 and Y_2 are replaced by the poorly adjoining cells Y_1 and Y_0. Of particular importance is the concentration of isolated Y cells (Y_0). The concentration of Y_0 (denoted by δx_2) is found to be 0.0412 at $x_2=0.55$. If these isolated cells Y_0 cease to contribute to the superconductivity, they can be incorporated into the nonsuperconducting group including Pr cells, as exhibited in Fig. 6. Therefore, the concentration $x_2=0.55$ becomes equivalent to the second percolation threshold x_{pc2} because of the concentration shift $\delta x_2=0.0412$: $x_2+\delta x_2 \approx 0.59=x_{pc2}$. The unisolated cells Y_1, Y_2, and Y_3 seem not to contribute to the concentration shift.

The above concentration shift means that each isolated Y cell is assimilated into the surroundings, namely, the adjacent Pr cells. This assimilation will result when the isolated Y cell loses its electronic identity by sharing the electron orbits in the CuO_2 plane with the adjacent Pr cells, which originally have a different type of electron orbits as implied by the $2p(O)-4f(Pr)$ orbital hybridization model by Fehrenbacher and Rice.[2] Above $x=0.55$, the Y_0 cells become crucial in forming the percolation cluster extending throughout the system, and hence the superconducting path is violated by the above assimilation of the Y_0 cells. In Fig. 2, the resistivity ρ for $x=0.55$ shows a distinct dependence on the current density J, while the J dependence is trivial for other concentrations $x=0.42$, 0.5, and 0.6. This observation implies that the superconducting path for $x>x_2$ almost vanishes because of the ineffective weak link between the Y_0 and either of the adjacent Y_n ($n\geqslant0$). This path structure will persist until x attains the second percolation threshold x_{pc2}.

If the above assimilation effect also acts on the isolated Pr cell (P_0), which is surrounded by the Y cells, the isolated Pr cell can add a contribution to the superconductivity with the aid of the adjacent Y cells; then the substantial first percolation threshold also varies. This situation will be viewed in Fig. 6 by exchanging the light and dark parts with each other and depicting P_0 in gray instead of Y_0. The incorporated concentration of P_0 at $x_1=0.44$ is read as $\delta x_1=0.043$ from Fig. 5; this value is equal to that of Y_0 at $x=0.56$, from the structural symmetry. Then, with this concentration shift δx_1, the point x_1 corresponds substantially to the first percolation

threshold x_{pc1}, since $x = x_1 - \delta x_1 \approx 0.40 \approx x_{pc1} = 0.41$. Therefore, a marked change in the structure of the superconducting path will occur at x_1 rather than at the true threshold x_{pc1}, as observed in Fig. 4.

Finally, as a possible origin of the thresholds x_1 and x_2, one may consider the concentration correction due to the substitution of Y and Pr for the Ba site.[4] However, the estimated correction of x was found to be too small and inconsistent when explaining both x_1 and x_2. It seems worth considering whether the threshold x_1 can be explained by the proximity effect for SNS junctions of YBCO-PBCO-YBCO,[9,10] since the narrow channel of PBCO becomes superconducting, giving an effect similar to the assimilation on the isolated Pr cells. If the extraordinarily large normal coherence length ξ_N as observed for these junctions (typically, $\xi_N \approx 30$ nm at 4.2 K) (Ref. 10) is valid in our samples, we should incorporate a PBCO cluster spanning the length ξ_N into the superconducting phase, and therefore, x_1 would take a value much larger than that estimated before. It is also to be noted that the proximity effect is dependent on T, because of ξ_N as a decreasing function of T. However, as described before, the threshold x_1 is almost independent of T up to 20 K, and therefore, this effect seems not to play a direct role in determining x_1. Another relevant issue is the problem of whether PBCO itself can be superconducting under particular conditions, as reported for a bulky crystal having lattice constants larger than the nonsuperconducting PBCO.[11] At present, it is uncertain whether the assimilation effect described so far has any reference to this superconducting conversion. However, it seems from this conversion that the electronic structure of PBCO is unstable, affected by chemical factors such as the lattice constants, the stoichiometry, or the presence of impurities, and such structural sensitivity will provide novel aspects of the percolation processes, as in the present study.

In conclusion, the superconducting path in YPBCO exhibits a nonclassical percolation behavior at temperatures as low as $T = 4.2$ K, which is characterized by the virtual thresholds $x_1 = 0.44$ and $x_2 = 0.55$, as follows: (1) for $x_{pc1} \geqslant x \geqslant 0$ the path is unaffected by h; (2) for $x_1 \geqslant x \geqslant x_{pc1}$ a precursory degradation of the path is seen, but the dependence on h is trivial; (3) for $x_2 \geqslant x \geqslant x_1$ the path largely depends on h, showing its fragility; (4) for $x_{pc2} \geqslant x \geqslant x_2$ the path almost vanishes; and (5) the insulator region $1 \geqslant x \geqslant x_{pc2}$. The presence of x_2 implies that the isolated Y cells are assimilated into the adjacent Pr cells, and hence x_2 appears as a virtual second percolation threshold corresponding to x_{pc2}. The above effect also acts on the isolated Pr cell, and hence it can contribute to the superconductivity by virtue of the adjacent Y cells. Therefore, the point x_1 is also a virtual threshold corresponding to the first percolation threshold x_{pc1}.

The author acknowledges the assistance of T. Goya (currently at Okin awa Electric Power Co. Ltd.) in the experiments.

[1] H. D. Jostarndt, U. Walter, J. Harnischmacher, J. Kalenborn, A. Severing, and E. Holland-Moritz, Phys. Rev. B **46**, 14 872 (1992).
[2] R. Fehrenbacher and T. M. Rice, Phys. Rev. Lett. **70**, 3471 (1993).
[3] L. Soderholm, K. Zhang, D. G. Hinks, M. A. Beno, J. D. Jorgensen, C. U. Segre, and I. K. Schuller, Nature (London) **328**, 604 (1987).
[4] B. Okai, M. Kosuge, H. Nozaki, K. Takahashi, and M. Ohta, Jpn. J. Appl. Phys., Part 2 **27**, L41 (1988).
[5] Y. X. Jia, J. Z. Liu, A. Matsushita, M. D. Lan, P. Klavins, and R. N. Shelton, Phys. Rev. B **46**, 11 745 (1992).
[6] M. Muroi and R. Street, Physica C **216**, 345 (1993).
[7] L. Govea, R. Escudero, D. Rios-Jara, C. Pina, F. Morales, C. Wang, and R. A. Barrio, Physica C **153**, 940 (1988).
[8] V. K. S. Shante and S. Kirkpatrik, Adv. Phys. **20**, 325 (1971).
[9] C. T. Rogers, A. Inam, M. S. Hegde, B. Dutta, X. D. Wu, and T. Venkatesan, Appl. Phys. Lett. **55**, 2032 (1989).
[10] T. Hashimoto, M. Sagoi, Y. Mizutani, J. Yoshida, and K. Mizushima, Appl. Phys. Lett. **60**, 1756 (1992).
[11] Z. Zou, K. Oka, T. Ito, and Y. Nishihara, Jpn. J. Appl. Phys., Part 2 **36**, L18 (1997).